Article

Not peer-reviewed version

PARP1: New Drug Development Opportunities for an Old Target

Pablo Iglesias , Marcos Seoane , Irene Golán-Cancela , Maximo Fraga , Víctor M. Arce , Jose A. Costoya *

Posted Date: 19 April 2023

doi: 10.20944/preprints202304.0530.v1

Keywords: Poly (ADP-Ribose) Polymerase-1; PARP inhibitors; neoplasm; cancer; animal disease models

Article

PARP1: New Drug Development Opportunities for an Old Target

Pablo Iglesias [1], Marcos Seoane [1], Irene Golán-Cancela [1], Maximo Fraga [2], Victor Arce [1] and Jose A. Costoya [1,*]

[1] Molecular Oncology Laboratory MOL, Departamento de Fisioloxia, CIMUS, Facultade de Medicina, Universidade de Santiago de Compostela, IDIS, Santiago de Compostela, Spain
[2] Departamento de Anatomia Patolóxica e Ciencias Forenses, Universidade de Santiago de Compostela, Santiago de Compostela, Spain
* Correspondence: josea.costoya@usc.es

Abstract: In recent years, new therapies have been developed based on molecules that target molecular mechanisms involved in both the initiation and maintenance of the oncogenic process. Among these molecules are the poly(ADP-ribose) polymerase 1 (PARP1) inhibitors. PARP1 has emerged as a target with great therapeutic potential for some tumor types, drawing attention to this enzyme and resulting in many small molecule inhibitors of its enzymatic activity. Thus, many PARP inhibitors are currently in clinical trials for the treatment of homologous recombination (HR)-deficient tumors, BRCA-related cancers, taking advantage of synthetic lethality. In addition, several novel cellular functions unrelated to its role in DNA repair have been described, including post-translational modification of transcription factors, or acting through protein-protein interactions as a co-activator or co-repressor of transcription. Previously, we reported that this enzyme may play a key role as a transcriptional co-activator of an important component of cell cycle regulation, the transcription factor E2F1. Here, we show that PARP inhibitors, which interfere with its activity in cell cycle regulation, do so without affecting its enzymatic function.

Keywords: poly(ADP-ribose) polymerase-1; PARP inhibitors; neoplasm; cancer; animal disease models

1. Introduction

As the cell cycle progresses, the cell divides and this division implies the duplication of its genetic material. Thus, the cell cycle is a highly regulated process that integrates many signals coming from the membrane, as well as from cellular pathways involved in controlling the genetic integrity to ensure the absence of genetic damage. The E2F/RB pathway is key to this regulation, and in fact mutations affecting this pathway induce an aberrant cell cycle activity and are highly associated with many types of cancer. The retinoblastoma tumor suppressor protein (RB) and the other "pocket protein" members, either p107 or p130, act as tumor suppressors through their important function as regulators of proliferation, differentiation, and apoptosis. The RB family exerts its role by interacting with many proteins, with E2F transcription factors being the best-characterized binding partners of RB. Activation of cyclin/CDKs complexes phosphorylates RB family members, decreasing their ability to interact with target proteins and thus altering their biological functions. Although eight E2F family members have been identified in mammals, only E2F1-6 have both a conserved DNA-binding domain and a dimerization domain, with E2F1-3 also containing an RB-binding sequence near the C-terminus [1]. Despite the sequence similarities among the Rb family members, RB preferentially binds to E2F1-4, this fact accounts for the fact that only RB mutations are frequently detected in cancers. In recent years, several reports have demonstrated that the E2F/RB pathway is regulated by independent cell cycle regulators including members of the poly(ADP-ribose) polymerase gene family. Currently, of the 17 identified members of the poly(ADP)-ribose) polymerase (PARP) family, most are enzymes capable of attaching poly(ADP-ribose) units to proteins or DNA using NAD^+ as a

 doi:10.20944/preprints202304.0530.v1

substrate [2]. Although PARP proteins have been classically implicated in DNA repair, several important functions have recently been identified, including cell division and transcriptional regulation. PARP1 regulates gene expression by various mechanisms, either through physical and direct functional interactions with chromatin, or by regulating the activity of chromatin regulating enzymes and transcriptional co-regulators [3–6].

Among these, PARP1 is known to alter gene expression by acting as either a co-activator or a co-repressor of transcription in a promoter-specific manner independent of its catalytic activity. Indeed, PARP1 can upregulate the transcriptional activity of E2F1 through its function as a co-activator during the re-entry of quiescent cells into S phase [7,8]. Recently, we have shown how PARP1 regulates the E2F1 transcriptional function through their interaction [9]. Here, we show how this transcriptional modulation can be affected by pharmacological treatment with PARP1-interacting molecules.

2. Results

2.1. In vitro effect of PARP inhibitors on the interaction of PARP1 and E2F1

The activity of the transcription factor E2F1, and in particular the G1/S transition, is strictly dependent on the phosphorylation of pRB. Thus, while a hypophosphorylated pRB is capable of binding and inhibiting E2F1, the hyperphosphorylation of this protein produces a series of allosteric changes that drastically modify their interaction, leaving the E2F1 factor free. This circumstance is used by a large number of tumor types that, by inactivating pRB, deregulate the activity of E2F1 and thus the cell cycle to their own advantage [10].

In a previous work [9], we have previously described that PARP1 acts as a co-activator of E2F1, and that its deficiency reduces the transcriptional activity of E2F1, thereby reducing tumor growth by decreasing E2F1 hyperactivation. Therefore, here we tested whether this decrease in E2F1 transcriptional activity could be achieved by using several representative examples of the different generations of chemical inhibitors of PARP1. Among the classical inhibitors, 3-aminobenzamide (Figure 1, compound 1) stands out as one of the first nicotinamide analogues used for this purpose [11]. Within the second generation we used derivatives of benzoquinolines and benzoquinolinones such as TiQ-A and PJ34 (Figure 1, compounds 3 and 4 respectively), and quinazolinones such as NU1025 (Figure 1, compound 2), which is the PARP1 inhibitor used in the pioneering synthetic lethality studies in BRCA1/2 deficient tumors [12,13]. Likewise, we also include one of the latest-generation inhibitors of PARP1, veliparib (ABT-888), that has demonstrated its efficacy in different clinical phase trials and in different tumor types [14,15]. Finally, we included gossypol (Figure 1, compound 6), a compound of natural origin with the ability to specifically block protein-protein interactions of PARP1 mediated by the central BRCT domain, as is the case with PARP1 and E2F1 [16].

Preprints (www.preprints.org) | NOT PEER-REVIEWED | Posted: 19 April 2023 doi:10.20944/preprints202304.0530.v1

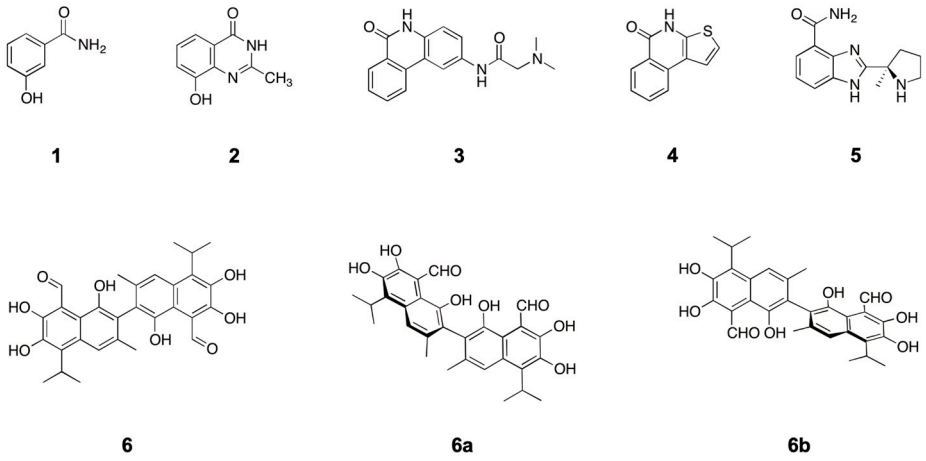

Figure 1. Structure of PARP1 inhibitors and gossypol, an inhibitor of PARP1 protein-protein interactions. Compound 1, 3-aminobenzamide; Compound 2, NU1025; Compound 3, PJ34; Compound 4, TiQ-A; Compound 5, ABT-888; Compound 6, gossypol. Gossypol was obtained from its natural source (cotton) as a racemic mixture of two atropisomers where the (-)-gossypol isomer (6a) specifically interferes with PARP1 protein-protein interactions.

To evaluate the effect the different PARP1 inhibitors on cell proliferation, we used mouse embryonic fibroblasts (MEFs) obtained from either Parp1$^{+/+}$ and Parp1$^{-/-}$ mice. Cells were seeded and serum-starved to maintain them in the G1/S transition, and then treated with the inhibitors. Cell proliferation was significantly decreased in Parp1$^{-/-}$, as compared with Parp1$^{+/+}$ and cells (Figure 2A), which is consistent with the role of PARP1 as a co-activator of E2F1 in the initiation of S phase. Interestingly, cell proliferation was also reduced after treatment of Parp1$^{+/+}$ cells with PARP1 inhibitors, more effectively in the case of cells treated with PJ34 or with gossypol (Figure 2B). Taken together, these data indicate that PARP1 inhibition significantly reduces E2F1 transcriptional activity and cell proliferation, consistent with the hypothesized contribution of PARP1 as a co-activator of this transcription factor. Chemical inhibition of the enzymatic activity of PARP1 has an effect similar to that observed in cells lacking this protein, whereas specific inhibition of the protein-protein interaction, as in the case of gossypol treatment, appears to have an even greater effect.

To further demonstrate the involvement of E2F transcriptional activity, we performed a luciferase activity assay using HEK293 cells transfected with the E2F-Luc vector and synchronized by the double thymidine method. Once released from arrest, cells were treated with the different inhibitors, as shown in Figure 2C. The enzymatic inhibition of PARP1 reduced the transcriptional activity of E2F1 in a manner similar to that of the PARP1 deficiency that we previously reported [9]. Within the experimental groups, we found that PJ34 is possibly the molecule, among the classical inhibitors of PARP1, that reduces this transactivation to a greater extent, while the luciferase activity is reduced by almost 40% compared with the untreated control in cells treated with gossypol.

To verify whether this effect on the transcriptional and proliferative activity correlates with the subcellular localization of the proteins, we co-transfected vectors containing the EGFP-PARP1 and RFP-E2F1 fusion proteins in HEK293 cells. These cells were maintained at the G1/S transition until treated with the inhibitors PJ34 and gossypol. Supplementary Figure S1A shows the co-localization of E2F1 and PARP1 in control cells, while treatment with the PJ34 inhibitor alters their subcellular localization, particularly of E2F1. At 4 and 6 hours, after treatment, the intensity of E2F1 decreases notably, suggesting that the stability of the transcription factor is somehow compromised (Supplementary Figure S1A). This is not the case for cells treated with gossypol (Supplementary Figure S1A), in which a slight delocalization that affects PARP1 to a greater extent is observed as soon

Preprints (www.preprints.org) | NOT PEER-REVIEWED | Posted: 19 April 2023 doi:10.20944/preprints202304.0530.v1

as after 4 hours of treatment. However, the possible side effects of gossypol treatment must be taken in consideration, since it is a mimetic of the BH3 domain of the anti-apoptotic protein Bcl-2. Therefore, gossypol can antagonize Bcl-2 function, which can lead to cell apoptosis [17,18]. Taking together, these data indicate an effect of PJ34 and, to a lesser extent gossypol, on the interaction between PARP1 and E2F1. This effect is consistent with the functional assays in which these treatments reduce the proliferation and transcriptional transactivation of treated cells.

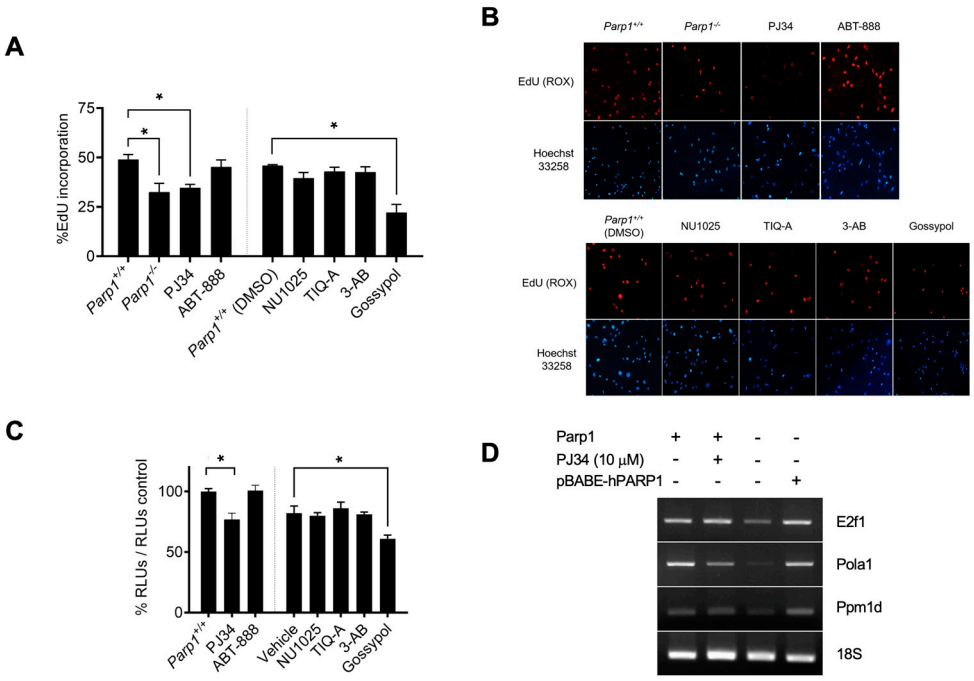

Figure 2. Effects of PARP1 inhibition on E2F1 transcriptional activity. A, EdU incorporation assay in MEF treated with the PARP1 inhibitors PJ34 (10 μM), ABT-888 (10 μM), NU1025 (100 μM), TIQ-A (50 μM), 3-AB (5 mM) and gossypol (25 μM). A vertical line separates cells treated with inhibitors dissolved in water and inhibitors dissolved in DMSO (*=p<0.01). B, representative images of results presented in panel A. Cell nuclei were counterstained with Hoechst 33258 (bisbenzimide). C, luciferase activity assay in HEK293 transfected with E2F-Luc plasmid treated with PARP-1 inhibitors. A vertical line separates cells treated with inhibitors dissolved in water and inhibitors dissolved in DMSO. Cells were synchronised prior to treatment, and results were normalized to its corresponding vehicle (water or DMSO). Shown is a representative experiment of three independent replicates (*=p<0.01) D, semiquantitative RT-PCR of E2F1 transcriptional targets. Results are representative from three independent experiment replicates.

Since the effects of PJ34 and gossypol treatments were observed in cells released from synchronization at the G1/S transition, we speculated that changes in the stability of the transcription factor E2F1 might be involved. Therefore, we treated cells expressing the fusion proteins with cycloheximide, which inhibits protein synthesis by blocking mRNA translation, and monitored protein stability. As can be seen in Supplementary Figure S1B, E2F1 levels vary very slightly in both control and gossypol-treated cells. In contrast, a pronounced variation is observed in cells treated with PJ34 after 6h of treatment, thus suggesting a possible effect of this molecule on the stability of E2F1.

To study the effect that the presence or absence of PARP1 could exert on the activity of E2F1, we also analyzed the mRNA levels of several genes regulated by E2F1 in fibroblasts, using semiquantitative PCR (RT-PCR). Our results show that the presence of PARP1 significantly reduces the transcriptional activity of the E2F1 protein, as well as other transcriptional targets of this factor, such as DNA polymerase α (Pola), whose induction occurs in early S phase, or the phosphatase Wip1

(Ppm1d). Indeed, the fact that we can rescue this effect by re-expressing a copy of PARP1 in Parp1$^{-/-}$ fibroblasts clearly demonstrates the role of PARP1 as a co-activator of the transcriptional activity of E2F1 (Figure 2D).

2.2. Chemical inhibition of PARP1/E2F1 interaction in a model of oncogenesis

As a final step in our study on the PARP1/E2F1 interaction, we investigated its possible consequences on oncogenesis. To this end, we took advantage of our model of gliomagenesis, based on the inactivation of a tumor suppressor (retinoblastoma) and the gain of function of an oncogene (HRas^{V12}) [19]. Since inactivation of retinoblastoma causes numerous cell cycle aberrations, mainly due to the uncontrolled behavior of E2F1, this model is an excellent test bench to study the effects of PARP1 in the context of hyperactivation of the E2F1 factor.

As we have already shown [9], Parp1$^{+/+}$ cRb$^{-/-}$ HRas^{V12} astrocytes obtained from P3 neonates present great heterogeneity in their shape and size, together with several morphological alterations, such as the presence of abundant cytoplasmic extensions. Loss of contact inhibition and formation of growth foci in the culture plates, which reflect the existence of a transformed phenotype, was also observed in these cells. In contrast, Parp1$^{-/-}$ cRb$^{-/-}$ HRas^{V12} astrocytes, display a similar phenotype, but lower cell density and a significantly decrease in the number of foci (Figure 3D). Altogether, these findings suggest that the degree of transformation is much lower in Parp1$^{-/-}$ cRb$^{-/-}$ HRas^{V12} astrocytes than in control cells. Interestingly, a similar effect, including a reduction in the number of foci was observed when Parp1$^{+/+}$ cRb$^{-/-}$ HRas^{V12} astrocytes were treated with the different PARP1 inhibitors (Figure 3A), especially in the case of PJ34 although these effects lower than in Parp1-deficient astrocytes. (Figure 3B).

To check whether this effect of PARP1 inhibitors on cell proliferation could be reflected in oncogene-induced senescence (OIS), we quantified the number of senescent cells in each experimental group using an SA-β-galactosidase activity assay (Figure 3C). Not surprisingly, the highest proportion of senescent cells, was observed in cells treated with PJ34, and to a lesser extent NU1025, which would explain their reduced proliferation compared to the rest of the experimental groups. Interestingly, we did not observe an increase in senescence in Parp1$^{-/-}$ astrocytes, which could be explained by an adaptive phenomenon induced by the chronic absence of PARP1. In contrast, no significant increase in apoptosis levels was observed in any experimental group (Supplementary Figure 1C).

In scenarios where there is DNA hyper-replication, for example due to the activation of an oncogene, the response to DNA damage is activated, leading to the appearance of oncogene-induced senescence (OIS). This mechanism of cellular defense depends on several checkpoints such as p16^{INK4a}, p21^{CIP1} and, most importantly, p53. This tumor suppressor constantly monitors the cellular stress and, if necessary, induces tumor suppressor signaling pathways, resulting in either cell arrest or cell apoptosis [20–24]. With this in mind, we wanted to see whether the morphological changes observed previously would be reflected in the proteins involved in the DNA damage checkpoints, and for this purpose we carried out an exhaustive biochemical analysis, which we present below in Figure 3E.

Regarding the status of the DDR checkpoints, a significant increase of activated p53 protein (p-p53^{S15}) was observed in virtually all groups treated with PARP1 inhibitors. This can be largely attributed to the inhibition of PARP enzymatic activity, which would potentiate the damage caused by the HRas^{V12} -induced DNA hyper replication. Interestingly, this damage-enhancing effect was not observed in astrocytes treated with ABT-888 and 3-AB (as reflected by phospho-histone H2AX levels), while phospho-histone H2AX levels were significantly reduced in the case of PJ34.

Preprints (www.preprints.org) | NOT PEER-REVIEWED | Posted: 19 April 2023 doi:10.20944/preprints202304.0530.v1

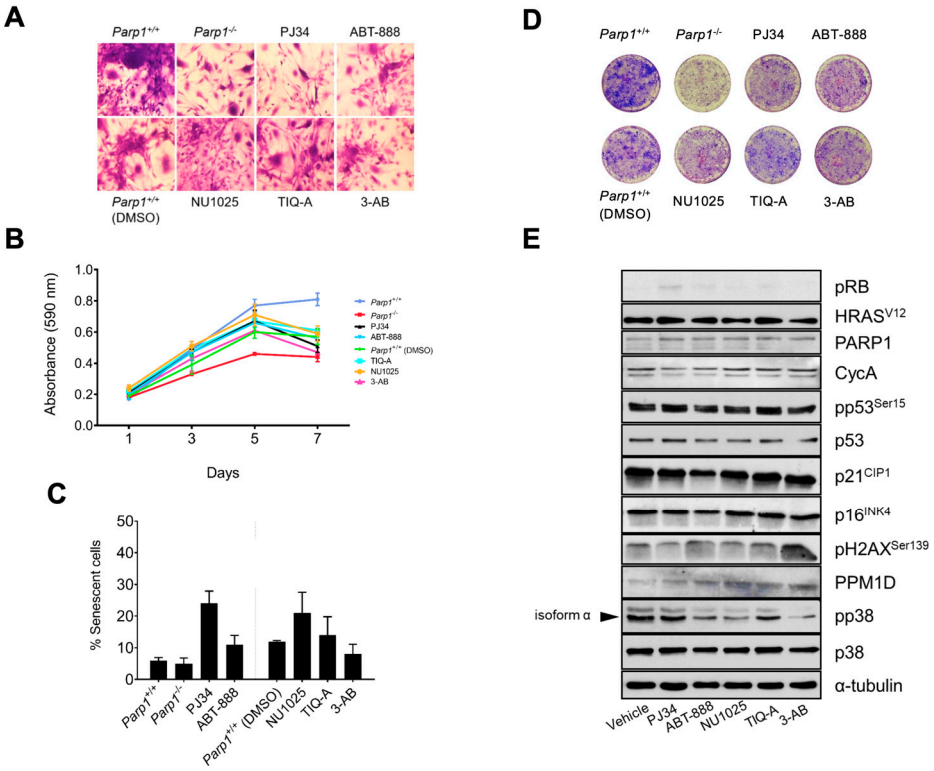

Figure 3. Effect of PARP1 inhibitors on primary astrocytes. Postnatal-day-3 astrocytes obtained from Parp1$^{-/-}$ cRb$^{-/-}$ HRas^{V12} or Parp1 +/+ cRb$^{-/-}$ HRas^{V12} mice were treated in vitro with PARP1 inhibitors. A, morphological changes in cells stained with crystal violet. B, proliferation rate. Cells were stained with crystal violet, and cell number was determined by spectrophotometry. C, percent of senescent cells, obtained by quantification of SA-β-galactosidase activity. D, colony formation. Astrocytes were fixed with methanol-acetic acid (3;1, v/v) and stained with 0.1% (w/v) crystal violet in PBS on day 7 of culture. D, biochemical analysis of the main checkpoints of the DNA damage response (DDR) as well as transcriptional targets of E2F1. All results are representative of, at least, three independent experiments.

On the other hand, if we observe the levels of the p21^{CIP1} cycle inhibitor, we see that these also increase in almost all the treated groups, which would explain the lower proliferation of these cells with respect to the untreated control. Regarding the transcriptional activity of E2F1, we observed two very important facts: first, the levels of cyclin A, a bona fide transcriptional target of E2F1, were reduced in cRb$^{-/-}$ HRas^{V12} astrocytes treated with PJ34. Second, the levels of phosphorylated p38 were higher in cells treated with PJ34, which may be related to the slightly decrease of Wip1 phosphatase (PPM1D), observed in PARP1-deficient astrocytes and in those treated with vehicle and PJ34. This finding may explain the higher level of senescence in PJ34-treated astrocytes, since downregulation of Wip1 on cRb$^{-/-}$ HRas^{V12} astrocytes sensitizes them to oncogene-induced senescence, as we previously reported [19].

In summary, our data demonstrate that chemical inhibition of PARP1, would increase DNA damage by blocking the enzymatic activity of PARP, involved in several mechanisms of DNA repair induced by replication stress. This increase in DNA damage, evidenced by the presence of high levels of phosphorylated p53, would rise the levels of p21 in the groups treated with inhibitors, thus increasing the percentage of senescent cells. In addition, in cells treated with PJ34, there is a lower transcriptional activity of E2F1, which is hyperactivated due to the deletion of pRb. This reduced activity of E2F1 translates into lower levels of the proteins regulated by this transcription factor: E2F1 itself, cyclin A, and Wip1, (Hershko et al., 2006). Dephosphorylation of p38MAPK by Wip1 greatly

Preprints (www.preprints.org) | NOT PEER-REVIEWED | Posted: 19 April 2023 doi:10.20944/preprints202304.0530.v1

reduces its activity, making astrocytes more susceptible to transformation. On the other hand, inactivation of Wip1 and consequent re-activation of p38MAPK restores the ability of the cells to enter senescence and reduce their proliferation rate [19,25].

2.3. Rescue from PARP1 deficiency

As a further demonstration of our previous experiments, investigated the effects of PARP1 inhibition by PJ34 treatment on the proliferation of PARP1-deficient cells in which a copy of hPARP1 was introduced by retroviral transduction. Supplementary Figure S2B–D, shows the effect of PARP1 inhibition with PJ34 on the proliferation and senescence in the different genotypes investigated in this experimental setting. As can be observed in Figure 4 the rescue of the PARP1-deficient phenotype, by re-expression of a copy of PARP1 has a small but appreciable effect on the proliferation in all cells expressing oncogenic Ras as well as in those deficient in pRb. The morphology of the knock-out astrocytes with re-expressed PARP1 should also be highlighted, since they show a more pronounced degree of transformation and, therefore, more similar to Parp1$^{+/+}$ astrocytes than to the control Parp1$^{-/-}$ (Figure 4A,B). On the contrary, while PARP1 re-expression does not appear to have a significant effect on astrocytes in terms of senescence, the level of apoptosis in Ras astrocytes is significantly reduced when a copy of PARP1 is present (Figure 4C,D). In this regard, we should also mention that in an a posteriori analysis the wild-type copy of PARP1 that we used in the present work incorporated a SNP, resulting in the substitution of alanine 762 by a valine residue. This mutation leads to an increase in Km for trans-poly(ADP-ribosyl)ation and results in a decrease in enzyme activity by approximately 50% [26]. However, this finding further supports the hypothesis that the reduction in proliferation observed in Parp1-deficient astrocytes is due to protein-protein interaction with E2F1.

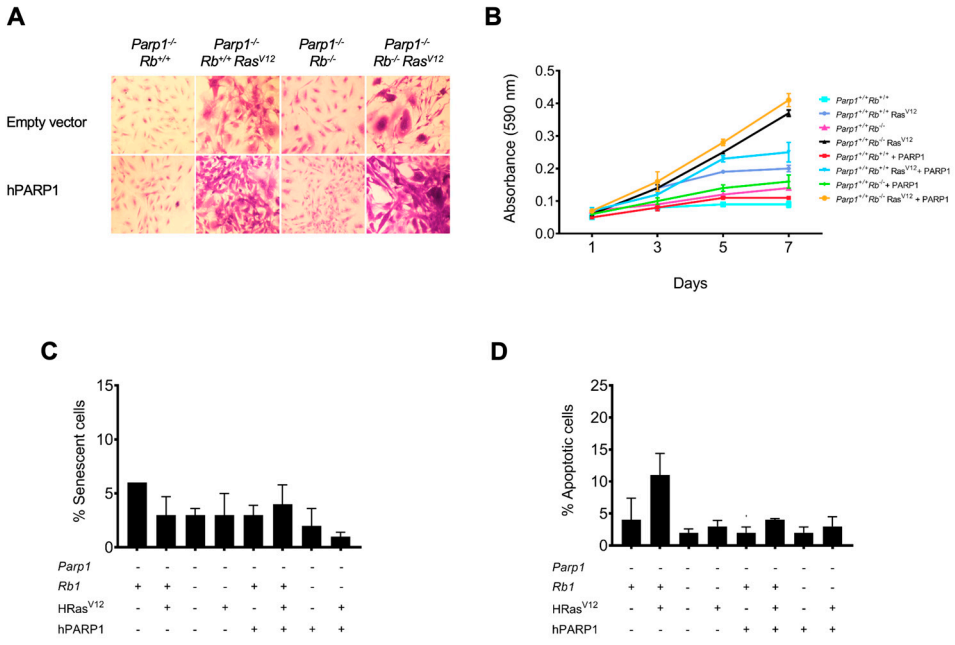

Figure 4. Effect of partially restoring of PARP1 catalytic activity. Primary astrocytes obtained from Parp1-/- cRb$^{flox/flox}$, Parp1-/- cRb$^{flox/flox}$ HRas^{V12}, Parp1$^{-/-}$ cRb$^{-/-}$, or Parp1$^{-/-}$ cRb$^{-/-}$HRas^{V12} mice were transduced with a copy of hPARP1 with reduced catalytic activity. A, morphological changes in cells stained with crystal violet. B, proliferation rate. Cells were stained with crystal violet, and cell number was determined by spectrophotometry. C, percent of senescent cells, obtained by quantification of SA-β-galactosidase activity. D, percent of apoptotic cells. Apoptotic nuclei were stained with Hoechst 33258. All results are representative of, at least, three independent experiments.

Preprints (www.preprints.org) | NOT PEER-REVIEWED | Posted: 19 April 2023 doi:10.20944/preprints202304.0530.v1

2.4. PARP inhibitors reduce tumor number and size in vivo

Finally, and to determine whether the transient inhibition of Parp1 could affect the transformation of modified astrocytes in vivo, we subcutaneously injected Parp1$^{+/+}$ cRb$^{-/-}$ HRas^{V12} astrocytes into the flank of the hindquarters of immunodeficient SCID mice (see Figure 5A for further details). As previously reported by our group [19], 100% of injected mice developed tumors. However, single intraperitoneal treatment with PJ34 (10 mg/kg) significantly reduced tumoral masses as compared to those injected with vehicle (Figure 5B–D). Histological analysis of the specimens (Figure 5E) also revealed a marked decrease in phosphorylated histone H3 labeling in the tumors obtained from treated mice.

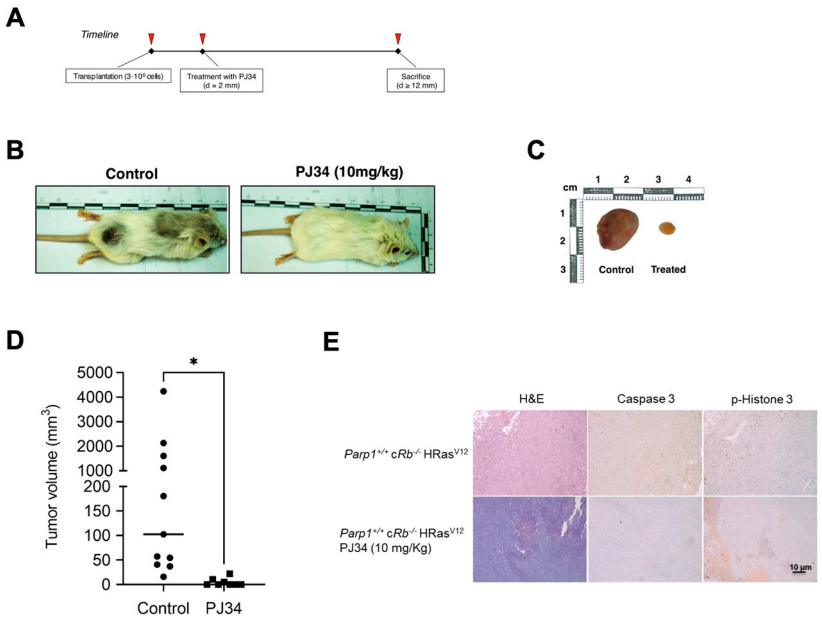

Figure 5. Effect of PARP-1 inhibition in vivo. A, timeline of the in vivo transformation assay. B, Effect of PJ34 on tumoral growth. Parp1$^{+/+}$ cRb$^{-/-}$ HRas^{V12} mice were injected subcutaneously with 3-10^6 astrocytes and treated with vehicle (control) or PJ34 (10 mg/kg). C, tumor volume in control (n=11) or PJ34-treated (n=8) mice (*=p<0.05). D, representative images or results presented in panel B. D, Caspase 3 and p-histone 3 expression in tumors obtained from control or PJ34-treated (n=8) mice.

3. Discussion

Functional inactivity of the tumor suppressor pRB present in various tumor types and transgenic animal models, leads to dysregulation of E2F1 transcriptional activity, which correlates with aberrant cell proliferation and, in some cases, with cell death [27–29]). The effects of Rb deficiency, or hyperactivation of E2F1, have been extensively studied both in relation to the initiation of the oncogenic process [10,30,31], and the induction of embryonic lethality in mice [32,33].

Based on studies by Simbulan-Rosenthal [7,8] and previous results from our group [9], we have shown that the PARP1 protein plays an important role in the transcriptional activity of E2F1 by modulating it at the G1/S transition. This modulation of E2F1 occurs through the direct interaction of both proteins and that in the case of PARP1 takes place through the central domain or self-modification which contains a BRCT motif like other proteins that interact with E2F1. In studies published by our group and others [8,9], it has been demonstrated that the association of PARP1 and E2F1 occurs directly on the promoter of E2F1 and other transcriptional targets of E2F1 such as cyclin A. Similarly, we also observed that the hyperactivation of E2F1 transcriptional activity in pRb-

Preprints (www.preprints.org) | NOT PEER-REVIEWED | Posted: 19 April 2023 doi:10.20944/preprints202304.0530.v1

deficient cells can be reduced if PARP1 is also absent, confirming the role of this protein as a co-activator of E2F1 [9].

Although this interaction does not seem to depend on the enzymatic activity of PARP1, since E2F1 is not poly(ADP-ribosyl)ated in vitro, we observed that treatment with an inhibitor reduces de the expression of some E2F1 transcriptional targets involved in the transition between low- and high-grade gliomas, such as POLA1 polymerase or WIP-1 phosphatase, in MEFs synchronized by serodeprivation [19,25]. Interestingly, a similar effect was observed when cells treated PJ34, a inhibitor of PARP1 enzymatic activity, and with gossypol, a molecule capable of specifically blocking the protein-protein interactions mediated by the BRCT motif of PARP1 [16].

Gossypol is a naturally occurring compound usually obtained as a racemic mixture of two stereoisomers of which only the (-)-gossypol isomer has the ability to interfere with PARP1 protein-protein interactions. Mechanistically, this biological activity translates into the ability of this molecule to react to form a Schiff base by reacting its two aldehyde functional groups with the amino groups of lysines 438 and 441 of the BRCT domain, thus blocking any possible interaction between PARP1 and other proteins.

In the case of PJ34, this molecule lacks aldehyde groups that allow a gossypol-like interaction with the BRCT domain of PARP1. As is well known, this inhibitor developed by Inotek [34], like many other PARP1 inhibitors, takes nicotinamide (NAM) as a structural model to bind to its binding site in the enzyme's catalytic center and block its activity. In addition to binding to the NAM pocket, this molecule can locate itself between the α-helix and the D-loop of tankyrase-1 (PARP-5a), both structural motifs that are also present in the domains of PARP1 catalytic agents, suggesting that, like PARP-5a, it is capable of binding two PJ34 molecules simultaneously at both binding sites [35].

In relation to these results, the assays with the EGFP-PARP1 and RFP-E2F1 fusion proteins not only confirm that the co-localization of PARP1 and E2F1 increases with time from the G1 to S phase, but in the case of cells treated with PJ34, the levels of the RFP-E2F1 fusion protein appear to decrease significantly. As seen below, in the same synchronized cells, whose protein translation had been inhibited by cycloheximide treatment, E2F1 levels decreased more sharply over time in the case of PJ34, suggesting that this inhibitor may affect the stability of E2F1.

Finally, we wanted to test whether this cooperation between both proteins also extends to an oncogenic context, which would allow us to modulate the activity of E2F1 by inhibiting PARP1. To do this, we used a model of gliomagenesis already characterized by our group, which is largely based on the hyperactivation of E2F1 by conditional deletion of pRb [19]. As in non-transformed cells, PARP1 inhibition leads to reduced proliferation, in addition to the reduction of aggressiveness and cell transformation observed in control cells (*Parp1*$^{+/+}$ *cRb*$^{-/-}$HRas^{V12}), especially in the case of PJ34. However, we also observed that in the case of cells treated with PJ34, the percentage of senescent cells in the culture increased (Figure 3C), which would also explain the lower proliferation rate of astrocytes treated with this inhibitor, in addition to the generation of fewer foci or colonies compared to untreated control astrocytes (Figure 3D). Consistent with this, the biochemical analysis shows an increase in the levels of the cycle inhibitor p21CIP as well as of phosphorylated p53 in the case of the group treated with PJ34, which would explain the increase in senescent cells observed in this group. Regarding this result, it is important to consider that PJ34, like the rest of the inhibitors used, may have some off-target or non-specific effects that could confound the results obtained. A review of the available literature shows that PJ34, in addition to presenting a high affinity for the catalytic centers of PARP1 and PARP-2, as expected since they are the ones with the greatest homology to each other, is also capable of binding to several members of its family (PARP-3, -4, -5a, -5b, -14, -16) [36], as well as the metalloprotease MMP-2 and the kinases PIM1 and PIM2, albeit with lower avidity [37]. Despite the apparent redundancy of the biological functions of the different PARPs, especially PARP1 and PARP-2, more and more specific functions are being discovered for these proteins [15,38,39]. Therefore, it is logical to speculate that the combined inhibition of multiple members of this family may have more durable and/or profound effects than the deletion of PARP1 alone and thus explain these differences between *Parp1*$^{-/-}$ *cRb*$^{-/-}$ HRas^{V12} and *Parp1*$^{+/+}$ *cRb*$^{-/-}$ HRas^{V12} treated with PJ34.

Also noteworthy, although expected, is the decrease in PPM1D (Wip1) and cyclin A levels in this group and in *Parp1*$^{-/-}$ *cRb*$^{-/-}$ HRas^{V12} cells, since both proteins are transcriptional targets of E2F1 itself. 1. Interestingly, the levels of p38-α kinase (MAPK14) were also increased in the case of PJ34 treatment in contrast to control cells. As we have already observed in previous studies in our laboratory, the level of oncogenesis-induced senescence (OIS) in *cRb*$^{-/-}$ HRas^{V12} astrocytes is closely related to the activity of the p38-α-specific phosphatase, Wip1. This phosphatase, once inactivated, allows p38 to activate and act as a brake on tumorigenesis by forcing astrocytes to slow down their proliferation and enter a senescent state [19,25]. In the same way, by reducing the transcriptional activity of E2F1, we also reduce the levels of Wip1 and therefore the proliferation of these cells that lack the protection of this phosphatase are affected by senescence mediated by oncogenes, and that in our case is HRas^{V12}.

To complement these results, we wanted to verify once again that the absence of PARP1 is responsible for the change in phenotype and aggressiveness of our astrocytes. In the results that we have presented previously, it can be clearly observed that the reintroduction of a copy of PARP1 with reduced catalytic activity increases the proliferation and the degree of transformation of *Parp1*$^{-/-}$ *cRb*$^{-/-}$ HRas^{V12} astrocytes, whereas, as in the previous experiment, the chemical inhibition of PARP1 by means of PJ34 has an antagonistic effect. We reached the same conclusion when injecting these astrocytes into SCID mice, since *Parp1*$^{-/-}$ *cRb*$^{-/-}$ HRas^{V12} cells had a very tumorigenic capacity compared to controls. In turn, a single-dose treatment (10 mg/kg) of the PJ34 inhibitor was sufficient to reduce the volume of the masses obtained in the treated mice. Finally, the immunohistological analysis of these tumor tissues confirmed that in the case of treatment with PJ34, proliferation is greatly reduced, as evidenced by the low labeling of phosphorylated histone H3 compared to control tissue. In the case of *Parp1*$^{-/-}$ *cRb*$^{-/-}$ HRas^{V12} astrocyte tumors, the labeling of proliferating cells was also reduced, but unlike what occurred in in vitro oncogenesis studies, the levels of cell apoptosis were reduced inside the tumor.

In conclusion, in the present study we have shown that treatment with the inhibitor PJ34 or the inhibitor of protein-protein interactions gossypol can reduce the transcriptional activity of E2F1 and the proliferation of the treated cells. Inhibition of PARP1 protects the cell against oncogenic stimuli by reducing its proliferative rate, both in vivo and in vitro, or by reactivating other cell signaling pathways involved in oncogenesis-induced senescence.

4. Materials and Methods

4.1. Primary Cell Cultures

Cells were maintained in Dulbecco's modified Eagle medium (Sigma-Aldrich, St. Louis, MO, USA) with 10% fetal bovine serum and 1% L-glutamine (GIBCO-Invitrogen, Waltham, MA, USA). Primary astrocytes were generated from both Parp1+/+ cRbloxP/loxP and Parp1−/− cRbloxP/loxP neonatal mice at P3. Oncogenic Ras expression and deletion of Rb was also achieved by retroviral transduction using Phoenix-Eco cells (Swift et al, 2001) transfected with pBABE, pBABE-HRasV12, PIG-puro, and PIG-CRE retroviral plasmids (a gift from P.P. Pandolfi). Transduced cells were selected by adding puromycin to the culture medium at 2 μg/mL.

4.2. PARP1 inhibition and other pharmacological treatments

The inhibitors 3-aminobenzamide (3-AB, sc-3501, Santa Cruz), NU 1025 (sc-203166, Santa Cruz), ABT-888 (sc-202901, Santa Cruz), TIQ-A (sc-204916, Santa Cruz) and PJ34 (528150, Sigma-Aldrich) were used to inhibit the catalytic activity of PARP1. In addition, an allosteric inhibitor of BRCT-mediated protein-protein interactions of PARP1, gossypol (G8761, Sigma-Aldrich), was also included in some of the experiments.

For the E2F-1 half-life assay, HEK293 cells were seeded in a 12-well multiwell plate at a density of 5-104 cells/cm2 and transfected with equimolar amounts of the pEGFP-PARP-1 (a gift from A. Chiarugi) and pRFP-E2F-1 (a gift from B. Su). After synchronisation with double-thymidine treatment, cells were released with fresh DMEM medium along with the treatments (PJ34 and

Preprints (www.preprints.org) | NOT PEER-REVIEWED | Posted: 19 April 2023 doi:10.20944/preprints202304.0530.v1

gossypol) and their respective controls plus cycloheximide (C7698, Sigma-Aldrich) at a final concentration of 35 μM.

4.3. Co-localization studies

For co-localization studies, 5 × 104 per cm2 HEK293 cells were seeded on EZ-multiwell slides (Millipore, Burlington, MA, USA). Cells were transfected using equimolar quantities of pEGFP-PARP1 (a gift from A. Chiarugi) and pRFP-E2F1 (a gift from B. Su) and synchronized by double thymidine treatment. Upon release from cell cycle block, cells were fixed with 2% paraformaldehyde (pH 7.4) and nuclei were counterstained using DAPI (Invitrogen, Waltham, MA, USA) and fluorescent images from three independent experiments were taken using a Leica TCS SP2 microscope.

4.4. Incorporation of 5-Ethynyl-2′-Deoxyuridine (EdU)

Mouse fibroblasts were seeded at 5000 cells per cm2 in 24-well plates. Culture medium was removed twenty-four hours later and replaced with low-serum medium (0.5% FCS). After 48 h, the starvation medium was replaced with high-serum medium (15% FCS) along with PARP1 inhibitors for 16 h and subsequently treated with 10 μM 5-ethynyl-2′-deoxyuridine (EdU) (Sigma-Aldrich) for two additional hours. Nuclei were stained using Hoechst 3358 (Sigma-Aldrich) and fluorescence images were collected from three different experiments.

4.5. Luciferase Assays

MEF were seeded in 12-well plates at 2500 cells per cm2. Cells were subsequently transfected with vectors pE2F-Luc (a gift from M. Collado) and pCMV-β-Gal (Clontech, Mountain View, CA, USA). The data from three independent experiments were normalized using beta-galactosidase activity.

4.6. Animal Studies

Xenografts were established in SCID (Severe Combined Immunodeficiency) mice aged 10 to 12 weeks. Cell implantation was carried out by subcutaneous injection in the hindquarters with 3 × 106 transduced astrocytes resuspended in 100 μL PBS 1×. Treatment with PJ34 (Sigma-Aldrich) was initiated once the tumor reached a minimum diameter of 2 mm with a single-dose of 10 mg/kg, injected intraperitoneally. Control animals were injected PBS in similar manner. All tumors included in the analysis reached a minimum diameter of 4 mm and mice were euthanized when they approached a maximum diameter of 12 mm. Tumors were considered ellipsoid in shape and their volume was calculated using the equation volume = 0.5 × (length × width) [40]. The conditional mouse strain for *Rb1* [41], was obtained from the Mouse Models of Human Cancer Consortium (MMHHC) repository. *Parp1*$^{-/-}$ strain [42] was a gift from Prof. de Murcia. All animal procedures were approved and performed according to the guidelines set out by the Institutional Ethics Committee for Animal Experimentation.

4.7. Immunoblot

Analysis of protein levels was carried out by immunoblot analysis of whole cell lysates using polyclonal antibodies against PARP1 (H-300, Santa Cruz), cyclin A (C-19, Santa Cruz), p53 (CM5, Novocastra), p-p53 ser15 (9284, Cell Signaling), p38 (C-20, Santa Cruz), p-p38 (Thr180/Tyr182) (sc-17852, Santa Cruz), p16 (M-156, Santa Cruz), p-H2AX Ser139 (07-164 Upstate), p21 (M-19, Santa Cruz), PPM1D/WIP1 (H-300, Santa Cruz) and E2F-1 (C-20, Santa Cruz), as well as monoclonal antibodies against pan-Ras-V12 (Ab-1, Calbiochem), cyclin D1 (DCS6, Cell Signaling), α-tubulin (T5168, Sigma-Aldrich), β-actin (MAB1501, Millipore), and Rb (554136, BD).

4.8. Immunohistochemistry

Analysis of fetal erythrocytes from cord blood samples was carried out by Wright-Giemsa staining. For immunohistochemical analysis, anti-cleaved caspase 3 (monoclonal, Cell Signaling) and phospho-histone H3 (polyclonal, Cell Signaling Technology, Inc) were used as primary antibodies. Immunohistochemical analysis was performed using a universal second antibody kit that uses a peroxidase-conjugated labelled dextran polymer (Envision Plus, Dako, Glostrup, Denmark). The following primary antibodies were used: anti-cleaved caspase 3 (monoclonal, Cell Signaling Technology, Inc) and phospho-histone H3 (polyclonal, Cell Signaling Technology, Inc).

4.9. Semiquantitative RT-PCR

Embryonic fibroblasts were seeded at a rate of 4-104 cells/cm2 in 10 cm plates and synchronized for 44 hours serodeprivation. Cells were released from arrest and left in factor-rich medium (DMEM 15% FBS) for 16 hours before RNA extraction. After obtaining the cDNA, specific sequences of each gene were amplified using the following oligonucleotide pairs: qE2F1-F 5′ CTCGACTCCTCGCAGATCG 3′, qE2F1-R 5′ AGCTCGGCGAGAAAAGAAATC3′, qPOLA1-F 5′ GAAGAACGAGATCAGCAG 3′, qPOLA1-R 5′ CCACATAGCCTATCCCATCGTC 3′, qWIP1-F 5′ GATGTATGTAGCGCATGTAGGTG 3′, qWIP1-R 5′ GTTCTGGCTTGTGATCTTGTGT 3′, 18S-F 5′ TTGACGGAAGGGCACCACCAG 3′, 18S-R 5′ CTCCTTAATGTCACGCACGATTTC 3′.

4.10. Statistics

Statistical analysis was performed with ANOVA and Student's t-test for multiple or simple comparisons, respectively. Tukey and Student–Neumel–Kaus tests were used for post-hoc analysis of ANOVA results. Mantel–Cox test was used to analyze Kaplan–Meier curves. In all cases, statistical significance was established at $p < 0.05$.

Supplementary Materials: The following supporting information can be downloaded at the website of this paper posted on Preprints.org, Supplementary Figure S1; Supplementary Figure S2.

Author Contributions: All authors have read and agree to the published version of the manuscript. Conceptualization, P.I., M.S. and J.A.C.; Data curation, V.M.A.; Formal analysis, P.I., I.G., M.F., V.M.A. and J.A.C.; Funding acquisition, J.A.C.; Investigation, P.I. and J.A.C.; Methodology, P.I., M.S., I.G., and M.F.; Project administration, J.A.C.; Supervision, J.A.C.; Validation, P.I. and M.S.; Writing, P.I., V.M.A. and J.A.C.

Funding: This work received financial support from the Ministerio de Ciencia e Innovación (PID2020-113501RB-I00; J.A.C.), the Consellería de Cultura, Educación e Ordenación Universitaria (GPC GI-1862, ED431B 2020/26 ; J.A.C. and V.M.A.). This work has received financial support from the Xunta de Galicia (Centro de investigación de Galicia accreditation 2019-2022; ED431G 2019/02) and the European Union (European Regional Development Fund – ERDF).

Institutional Review Board Statement: All animal procedures were approved and performed according to the guidelines set out by the USC Bioethics Board (protocol No 15005AE/07/FUN01/FIS02/JACP1

Acknowledgments: The authors thank the members of Molecular Oncology Laboratory for the helpful discussions.

Conflicts of Interest: The authors declare no conflict of interest.

References

1. Du, W, Pogoriler, J. Retinoblastoma family genes. *Oncogene* **2006,** 25:5190-200
2. Ji, Y, Tulin, A.V. The roles of PARP1 in gene control and cell differentiation. *Curr Opin Genet Dev.* **2010** 20:512-8. doi: 10.1016/j.gde.2010.06.001. .
3. D'Amours, D., Desnoyers, S., D'Silva, I., Poirier, G.G.. Poly(ADP-ribosyl)ation reactions in the regulation of nuclear functions. *Biochem J.* **1999**, 342, 249-268.
4. Kraus, W.L , Lis, J.T. PARP goes transcription. *Cell*. **2003**, 113, 677-683
5. Kraus, W.L. Transcriptional control by PARP-1: chromatin modulation, enhancer-binding, coregulation, and insulation. *Curr Opin Cell Biol*. **2008**, 20, 294-302
6. Krishnakumar, R., Kraus, W.L. PARP-1 regulates chromatin structure and transcription through a KDM5B-dependent pathway. *Mol Cell*. **2010**, 39, 736-749

7. Simbulan-Rosenthal, C.M, Rosenthal, D.S, Luo, R., Smulson, M.E . Poly(ADP-ribose) polymerase upregulates E2F-1 promoter activity and DNA pol alpha expression during early S phase. *Oncogene*. **1999**, 18, 5015-5023
8. Simbulan-Rosenthal, CM, Rosenthal, D.S., Luo, R., Samara, R., Espinoza L.A., Hassa, P.O, Hottiger, M.O., Smulson, M.E.. PARP-1 binds E2F-1 independently of its DNA binding and catalytic domains, and acts as a novel coactivator of E2F-1-mediated transcription during re-entry of quiescent cells into S phase. *Oncogene*. **2003**, 22, 8460-8471.
9. Iglesias, P., Seoane, M., Golán, I., Castro-Piedras, I., Fraga, M, Arce, V.M, Costoya, J.A. PARP1 Deficiency Reduces Tumour Growth by Decreasing E2F1 Hyperactivation: A Novel Mechanism in the Treatment of Cancer. *Cancers (Basel)*. **2020**, 12:2907. doi: 10.3390/cancers12102907.
10. Malumbres, M., Barbacid, M. To cycle or not to cycle: a critical decision in cancer. *Nat Rev Cancer*. **2001** Dec;1(3):222-31.
11. Shall, S. Proceedings: Experimental manipulation of the specific activity of poly(ADP-ribose) polymerase. *J Biochem*. **1975**, 77(1): 2p.
12. Farmer, H., McCabe, N., Lord, C.J., Tutt, A.N., Johnson, D.A., Richardson, T.B., Santarosa, M., Dillon, K.J., Hickson, I., Knights, C., Martin, N.M., Jackson, S.P., Smith, G.C., Ashworth, A. Targeting the DNA repair defect in BRCA mutant cells as a therapeutic strategy. *Nature*. **2005**, 434:917-921.
13. Bryant, H.E., Schultz, N., Thomas, H.D., Parker, K.M., Flower, D., Lopez, E., Kyle, S., Meuth, M., Curtin, N.J., Helleday, T. Specific killing of BRCA2-deficient tumours with inhibitors of poly(ADP-ribose) polymerase. *Nature*. **2005**, 434: 913-917.
14. Davar, D., Beumer, J.H., Hamieh, L., Tawbi, H. Role of PARP inhibitors in cancer biology y therapy. *Curr Med Chem*. **2012**, 19:3907-3921.
15. Iglesias, P., Costoya, J.A. The antimitotic potential of PARP inhibitors, an unexplored therapeutic alternative. *Curr Top Med Chem*. **2014**, 14:2346-2365.
16. Na, Z., Peng, B, Ng, S., Pan, S., Lee, J.S., Shen, H.M., Yao, S.Q. A Small-Molecule Protein-Protein Interaction Inhibitor of PARP1 That Targets Its BRCT Domain. *Angew Chem Int Ed Engl.* **2015**, 54:2515-2519.
17. Oliver, C.L., Bauer, J.A,, Wolter, K.G., Ubell, M.L., Narayan, A., O'Connell, K.M., Fisher, S.G., Wang, S., Wu, X., Ji, M,, Carey, T.E., Bradford, C.R. In vitro effects of the BH3 mimetic, (-)- gossypol, on head y neck squamous cell carcinoma cells. *Clin Cancer Res.* **2004**, 10:7757-7763.
18. Chonghaile, T., Letai, A. Mimicking the BH3 domain to kill cancer cells. *Oncogene*. **2009**, Suppl 1:S149-57.
19. Seoane, M., Iglesias, P., Gonzalez, T., Dominguez, F., Fraga, M., Aliste, C., Forteza, J., Costoya, J.A. *PLoS One*. **2008**, 3:e3632.
20. Bartkova, J., Horejsí, Z,, Koed, K., Krämer, A., Tort, F., Zieger, K., Guldberg, P., Sehested, M., Nesland, J.M., Lukas, C., Ørntoft, T., Lukas, J., Bartek, J. DNA damage response as a candidate anti-cancer barrier in early human tumorigenesis. *Nature*. **2005**, 434(7035):864-870.
21. Bartkova, J., Rezaei, N., Liontos, M., Karakaidos, P., Kletsas, D., Issaeva, N., Vassiliou, L.V., Kolettas, E., Niforou, K., Zoumpourlis, V.C., Takaoka, M., Nakagawa, H., Tort, F., Fugger, K., Johansson, F., Sehested, M., yersen, C.L., Dyrskjot, L,, Ørntoft, T., Lukas, J., Kittas, C., Helleday, T., Halazonetis, T.D., Bartek, J., Gorgoulis, V.G. Oncogene-induced senescence is part of the tumorigenesis barrier imposed by DNA damage checkpoints. *Nature*. **2006,** 444:633-637.
22. Collado, M., Gil, J., Efeyan, A., Guerra, C., Schuhmacher, A.J., Barradas, M., Benguría, A., Zaballos, A., Flores, J.M., Barbacid, M., Beach, D., Serrano, M. Tumour biology: senescence in premalignant tumours. *Nature*. **2005**, 436:642.
23. Di Micco, R., Fumagalli, M., Cicalese, A., Piccinin, S., Gasparini, P., Luise, C., Schurra, C., Garre', M., Nuciforo, P.G., Bensimon, A., Maestro, R., Pelicci, P.G., d'Adda di Fagagna, F. Oncogene-induced senescence is a DNA damage response triggered by DNA hyper-replication. *Nature*. **2006**, 444:638-642.
24. Dolado, I., Swat, A., Ajenjo, N., De Vita, G., Cuadrado, A., Nebreda, A.R. p38alpha MAP kinase as a sensor of reactive oxygen species in tumorigenesis. *Cancer Cell.* **2007**, 11:191-205.
25. Bulavin, D.V., Phillips, C., Nannenga, B., Timofeev, O., Donehower, L.A., Anderson, C.W., Appella, E., Fornace, A.J. Jr. Inactivation of the Wip1 phosphatase inhibits mammary tumorigenesis through p38 MAPK-mediated activation of the p16(Ink4a)-p19(Arf) pathway. *Nat Genet*. **2004** 36:343-350. doi: 10.1038/ng1317.
26. Wang, X.G., Wang, Z.Q., Tong, W.M., Shen, Y. PARP1 Val762Ala polymorphism reduces enzymatic activity *Biochem Biophys Res Commun.* **2007**, 354:122-126.
27. DeGregori, J., Johnson, D.G. Distinct y Overlapping Roles for E2F Family Members in Transcription, Proliferation y Apoptosis. *Curr Mol Med*. **2006**, 6:739-748.
28. Iaquinta, P.J., Lees, J.A. Life y death decisions by the E2F transcription factors. *Curr Opin Cell Biol.* **2007**, 19:649-657.
29. Dimova, D.K., Dyson, N.J. The E2F transcriptional network: old acquaintances with new faces. *Oncogene*. **2005**, 24:2810-2826.

30. Bosco, E.E., Knudsen, E.S. RB in breast cancer: at the crossroads of tumorigenesis y treatment. *Cell Cycle*, **2007**, 6:667-671.
31. Knudsen, E.S., Knudsen, K.E. Tailoring to RB: tumour suppressor status y therapeutic response. *Nat Rev Cancer*. **2008**, 8:714-724.
32. Jacks, T., Fazeli, A., Schmitt, E.M., Bronson, R.T., Goodell, M.A., Weinberg, R.A. Effects of an rb mutation in the mouse. *Nature*. **1992**, 359:295-300.
33. Wu, L., de Bruin, A., Saavedra, H.I., Starovic, M., Trimboli, A., Yang, Y., Opavska, J., Wilson, P., Thompson, J.C., Ostrowski, M.C., Rosol, T.J., Woollett, L.A., Weinstein, M., Cross, J.C., Robinson, M.L., Leone, G. Extra-embryonic function of Rb is essential for embryonic development y viability. *Nature*. **2003**, 421:942-947.
34. Abdelkarim, G.E., Gertz, K., Harms, C., Katchanov, J., Dirnagl, U., Szabó, C., Endres, M. Protective effects of PJ34, a novel, potent inhibitor of poly(ADP-ribose) polymerase (PARP) in in vitro y in vivo models of stroke. *Int J Mol Med*. **2001**, 7:255-260.
35. Ekblad, T., Camaioni, E., Schüler, H., Macchiarulo, A. PARP inhibitors: polypharmacology versus selective inhibition. *FEBS J*. **2013**, 280:3563-3575.
36. Wahlberg, E., Karlberg, T., Kouznetsova, E., Markova, N., Macchiarulo, A., Thorsell, A.G., Pol, E., Frostell, Å., Ekblad, T., Öncü, D., Kull, B., Robertson, G.M., Pellicciari, R., Schüler, H., Weigelt, J. Family-wide chemical profiling y structural analysis of PARP y tankyrase inhibitors. *Nat Biotechnol.* **2012**, 30(3):283-8.
37. Antolín, A.A., Jalencas, X., Yélamos, J., Mestres, J. Identification of pim kinases as novel targets for PJ34 with confounding effects in PARP biology. *ACS Chem Biol.* **2012**, 7:1962-1967.
38. Yélamos, J., Schreiber, V., Dantzer, F. Toward specific functions of poly(ADP- ribose) polymerase-2. *Trends Mol Med*. **2008**, 14:169-178. doi: 10.1016/j.molmed.2008.02.003.
39. Hsiao, S.J., Smith, S. Tankyrase function at telomeres, spindle poles, y beyond. *Biochimie*. **2008**, 90:83-92.
40. Euhus, D.M.; Hudd, C.; LaRegina, M.C.; Johnson, F.E. Tumor measurement in the nude mouse. J. Surg. Oncol. 1986, 31, 229-234.
41. Marino, S.; Vooijs, M.; Van Der Gulden, H.; Jonkers, J.; Berns, A. Induction of medulloblastomas in p53-null mutant mice by somatic inactivation of Rb in the external granular layer cells of the cerebellum. Genes Dev. 2000, 14, 994-1004.
42. De Murcia, J.M.; Niedergang, C.; Trucco, C.; Ricoul, M.; Dutrillaux, B.; Mark, M.; Oliver, F.J.; Masson, M.; Dierich, A.; LeMeur, M.; et al. Requirement of poly(ADP-ribose) polymerase in recovery from DNA damage in mice and in cells. Proc. Natl. Acad. Sci. USA 1997, 94, 7303-7307.